A New Energy-free Gravity-compensation Adaptive System for Balancing of 4-DOF Robot Manipulators with Variable Payloads

Sébastien Briot, Vigen Arakelian

A New Energy-free Gravity-compensation Adaptive System for Balancing of 4-DOF Robot Manipulators with Variable Payloads

S. Briot* and V. Arakelian†

Institut de Recherche en Communications et Cybernétique de Nantes (IRCCyN)
UMR CNRS 6597, Nantes, France

Abstract—*In most of gravity balancing approaches devoted to robot manipulators, the gravity compensation is carried out for cancelling of the static efforts due to robot element masses, as well as a fixed payload. When the payload is variable, i.e. if for each cycle of the robot operation it is different, the known compensation techniques are not efficient. Some solutions permitting to compensate the gravity effects of variable payloads have been developed. However, they have similar drawbacks. To adapt the robot to the changing payload it is necessary: i) to increase the number of actuators and ii) to bring energy inside the system, i.e. the adaption technique is not energy efficient.*

This paper deals with a new gravity-compensation system for cancellation of the static loads of the changing payload. It is shown that the adaption to a new manipulated payload does not need to bring energy inside the system, i.e. the adaption technique is energy efficient. Simulations of the suggested mechanism by using ADAMS software are performed and show the efficiency of the proposed solution.

Keywords: robot manipulators, gravity compensation, static balancing, variable payload

I. Introduction

Any mechanism is statically balanced (also denoted as gravity-balanced) if its potential energy is constant for all possible configurations. With regard to the static balancing in robotics, this term differs from the first definition because in this case, the aim of the balancing is the minimization or cancellation of input efforts of a mechanical system by means of gravitational force balancing. This means that the mechanism is statically stable for any configuration; i.e., zero actuator input efforts due to the static loads are required.

For static balancing of robot mechanisms, different approaches and solutions have been developed and documented. The balancing schemes for robotic systems can be systematized by taking into account the nature of the compensation force:

- with counterweights (group A): this is a classical approach which consists in adding counterweights in order to keep the total centre of mass of moving links stationary [1–9].
- with spring (group B): the approaches developed in this group are based on the use of either zero-free length springs or non zero-free length springs [10–25].
- with a complementary actuator which can be a pneumatic or hydraulic cylinder, electromagnetic device, etc. (group C): In this case, a pneumatic or hydraulic cylinder is connected with some manipulator links [26–29] or directly with the moving platform [30]. There are also some approaches based on special counterweights, which are fluid reservoirs. Continuous gravity compensation is achieved by the pumping of fluid from the first reservoir-counterweight to the second.

The main drawbacks of the mentioned solutions when applied to robotics is that they ensure the gravity balancing of the robot for a given gravity load. However, when this load is varying (for example, during a palletizing task), they cannot ensure the cancellation of the gravity effects due to change of the payload. To overcome this difficulty, a few solutions have been proposed. The most resourceful ones are listed below:

- The use of active counterweights, such as in [28, 31] where the position of the counterweights on the balanced links varies and is modified through the use of additional actuators. This leads to the increase of the number of actuators and, obviously, to the development of a more complex controller.
- In [32], a variable gravity compensation mechanism is proposed. It uses two types of linear springs and changes the equilibrium position of one of these. This also leads to the considerable increase of the number of actuators and the achievement of more complex controllers.
- The gravity compensation technique developed in [33–35] uses remote counterweights connected to the robot via a hydraulic transmission. As it has been shown in [34] the built prototype of the 7-degrees-of-freedom (*DOF*) robot is able to adapt its balancing counterweights to a payload of up to 10 kg, which was a maximal payload for the tested prototype. The main drawbacks of this technique is the use of hydraulic power systems (while the robot energy is provided by electricity) and the increase of the system footprint.

An additional drawback of all these techniques is the fol-

*Sebastien.Briot@irccyn.ec-nantes.fr
†vigen.arakelyan@insa-rennes.fr

(a)The Kuka KR 700 PA (courtesy of Kuka)

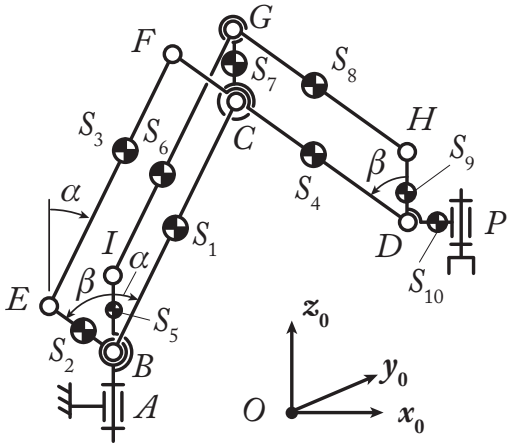

(b)Its kinematic architecture

Fig. 1. The Kuka KR 700 PA able to carry out variable payloads up to 700 kg.

lowing. When the payload is changing from a mass m_1 to a mass m_2, there is a change of potential energy in the system equal to $\Delta V = gz(m_2 - m_1)$ (where g is the gravitational constant and z the altitude at which the load is changed). Therefore, if $m_2 > m_1$, energy must be brought in the system to be able to adapt and to compensate the new payload. If $m_2 < m_1$, if the robot was ideal, it should be able to stock the non necessary energy in capacitors or batteries. However, even if most robot actuators are now equipped with four-quadrant amplifiers which are able to stock additional energy in capacitors, as the stocking performance of capacitors is limited, many energy is still dissipated (under the form of heat) to avoid the overload of the capacitors.

Thus, all existing adaptive gravity-compensation systems of robots are not energy efficient. Please note that the energy efficiency of machines (but not only machines) in EU will becomes soon an important research problem as the actual european policy is to target a decrease of 20% of consumed energy for 2020 (and 40% for 2030). In the present paper, taking into account that many robots used for the pick-and-place operations of heavy devices (such as palletization operations) are 4-*DOF* industrial robots such as the Kuka KR 700 PA presented in Fig. 1, we present an active balancing system able to compensate the gravity effects of a variable payload without the need of bringing additional energy in the whole robotic system. In the Section II, we show that it is possible to fully balance the gravity effects on the manipulator. Then, in Section III, we present the adaptive-gravity balancing system able to compensate the gravity effect of variable payloads. In Section IV, numerical validations made with the software ADAMS are performed. Finally, in Section V, conclusions are drawn.

It should be noticed that a patent on the proposed balancing system is currently pending [36].

II. Gravity-balacing of the manipulator only

A. Description of the robot architecture to balance without payload

Let us consider the kinematic architecture of the 4-*DOF* industrial robot depicted at Fig. 1(b). This architecture, made of revolute (*R*) joints only, allows the robot to perform Schönflies motions (i.e. its effector located at point P is able to carry out three translations along the base frame axes $\boldsymbol{x}_0$, $\boldsymbol{y}_0$ and $\boldsymbol{z}_0$ and one rotation around $\boldsymbol{z}_0$). These four *DOF* are controlled through the actuation of motors linked to the *R* joints located at points A, B (two *R* joints are located at this point, one controlling the angle α, the second one the angle β) and P.

The links attached to the *R* joints located at:
- B, C, F and E,
- B, C, G and I,
- C, D, H and G,

form articulated planar parallelograms (also denoted as Π joints). The Π joints $BCGI$ and $CDHG$ ensure the axis of the *R* joints located at point P to be always vertical, while the Π joint $BCFE$ allows for remoting the actuation of the link CD as close as possible to the base.

In the following of the paper, the gravity field $\mathbf{g}$ is equal to $\mathbf{g}= [0\ 0\ -g]^T$ ($g > 0$) and is directed along $\mathbf{z}_0$. Moreover, we denote as:
- S_i the centre of mass of the link i,
- m_i the mass of the link i,
- ℓ_{QR} the length between two arbitrary points Q and R,
- z_Q the position along the $\mathbf{z}_0$ axis of anarbitrary point Q.

B. Computation of the gravitational potential energy

The robot (without payload) gravitational potential energy V is given by:

$$V = g\sum_{i=1}^{10} m_i z_{S_i} \tag{1}$$

in which

$$z_{S_1} = z_B + \ell_{BS_1}\cos\alpha \quad (2)$$
$$z_{S_2} = z_B + \ell_{BS_2}\cos\beta \quad (3)$$
$$z_{S_3} = z_B + \ell_{BE}\cos\beta + \ell_{ES_3}\cos\alpha \quad (4)$$
$$z_{S_4} = z_B + \ell_{BC}\cos\alpha - \ell_{CS_4}\cos\beta \quad (5)$$
$$z_{S_5} = constant \quad (6)$$
$$z_{S_6} = z_I + \ell_{IS_6}\cos\alpha \quad (7)$$
$$z_{S_7} = z_B + \ell_{BC}\cos\alpha + l_{CS_7} \quad (8)$$
$$z_{S_8} = z_B + \ell_{BC}\cos\alpha + l_{CG} - \ell_{GS_8}\cos\beta \quad (9)$$
$$z_{S_9} = z_B + \ell_{BC}\cos\alpha - \ell_{CD}\cos\beta + \ell_{DS_9} \quad (10)$$
$$z_{S_{10}} = z_B + \ell_{BC}\cos\alpha - \ell_{CD}\cos\beta \quad (11)$$

taking into account that z_B and z_I have constant values.

Introducing (2)–(11) into (1), and simplifying, we obtain

$$V = a\cos\alpha + b\cos\beta + c \quad (12)$$

with

$$a = g(m_1\ell_{BS_1} + m_3\ell_{ES_3} + m_4\ell_{BC} + m_6\ell_{IS_6}) + g(m_7\ell_{BC} + m_8\ell_{BC} + m_9\ell_{BC} + m_{10}\ell_{BC}) \quad (13)$$

$$b = g(m_2\ell_{BS_2} + m_3\ell_{BE} - m_4\ell_{CS_4} - m_8\ell_{GS_8}) - g(m_9\ell_{CD} + m_{10}\ell_{CD}) \quad (14)$$

$$c = g\,z_B(\sum_{i=1}^{4} m_i + \sum_{i=7}^{10} m_i) + g(m_5 z_{S_5} + m_6 z_I) + g(m_7 l_{CS_7} + m_8 l_{CG} + m_9 \ell_{DS_9}) = const \quad (15)$$

C. Balancing of the manipulator

The gravity balancing of the manipulator will be achieved if and only if the potential energy becomes constant. For that, two usual methods are possible:

- the addition of two counterweights on links BC and EB (Fig. 2(a)),
- the addition of two zero-free length springs on links BC and EB (Fig. 2(b)).

C.1 Balancing of the manipulator by adding counterweights

Let us denote as (Fig. 2(a)):

- m_{cw1} the mass of the counterweight on link BC which is located at the distance r_{cw1} of the *R* joint at point B,
- m_{cw2} the mass of the counterweight on link EB which is located at the distance r_{cw2} of the *R* joint at point B.

The potential energy V_{cw} of the counterweights is given by:

$$V_{cw} = -g(m_{cw1}r_{cw1}\cos\alpha + m_{cw2}r_{cw2}\cos\beta) \quad (16)$$

The total potential energy $V + V_{cw}$ is thus constant (i.e. the robot is gravity-balanced) if and only if the counterweights are designed such that:

$$m_{cw1} = a/(g\,r_{cw1}) \quad (17)$$
$$m_{cw2} = b/(g\,r_{cw2}) \quad (18)$$

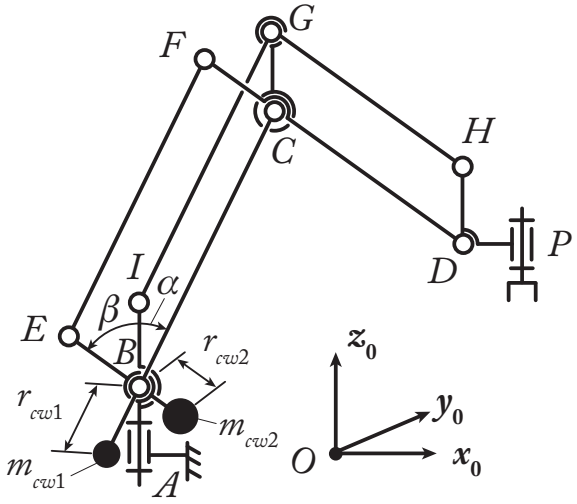

(a)

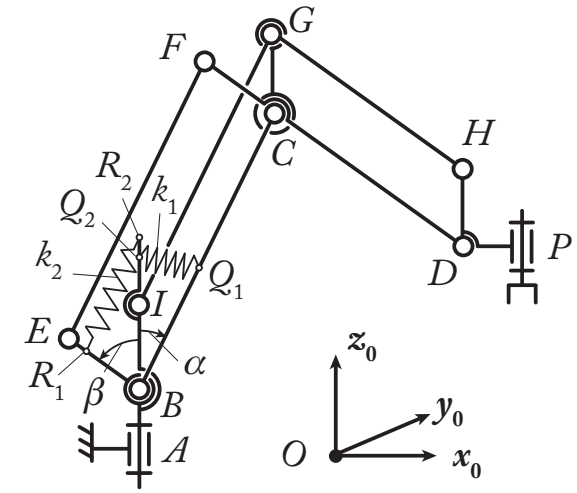

(b)

Fig. 2. Balancing of the robot manipulator under consideration. (a) via counterweights, (b) via zero-free length springs

C.2 Balancing of the manipulator by adding zero-free length springs

Let us denote as (Fig. 2(b)):

- k_1 the stiffness of the spring on link BC acting between the points Q_1 and Q_2,
- k_2 the stiffness of the spring on link EB acting between the points R_1 and R_2.

The potential energy V_{sp} of the zero-free length springs is given by:

$$V_{sp} = \frac{k_1\ell^2_{Q_1Q_2} + k_2\ell^2_{R_1R_2}}{2} \quad (19)$$

Noting the fact that:

$$\ell_{Q_1Q_2}^2 = \ell_{BQ_1}^2 + \ell_{BQ_2}^2 - 2\ell_{BQ_1}\ell_{BQ_2}\cos\alpha \quad (20)$$

$$\ell_{R_1R_2}^2 = \ell_{BR_1}^2 + \ell_{BR_2}^2 - 2\ell_{BR_1}\ell_{BR_2}\cos\beta \quad (21)$$

and introducing it into (19), we get:

$$V_{sp} = -k_1\ell_{BQ_1}\ell_{BQ_2}\cos\alpha - k_2\ell_{BR_1}\ell_{BR_2}\cos\beta + d \quad (22)$$

where d is a constant equal to

$$d = \frac{k_1(\ell_{BQ_1}^2 + \ell_{BQ_2}^2) + k_2(\ell_{BR_1}^2 + \ell_{BR_2}^2)}{2} \quad (23)$$

The total potential energy $V + V_{sp}$ is thus constant (i.e. the robot is gravity-balanced) if and only if the springs are designed such that:

$$k_1\ell_{BQ_1}\ell_{BQ_2} = a \quad (24)$$

$$k_2\ell_{BR_1}\ell_{BR_2} = b \quad (25)$$

Now that we have considered the balancing of the robot, let us consider the balancing of the variable payload.

III. Adaptive gravity-balacing system

In the following of this Section, we consider that the robot manipulator is self-balanced using one of the method proposed in the previous Section (the balancing solutions will not be drawn on the following pictures for reason of drawing clarity) and we only focus on the balancing of the variable payload.

A. Description of the adaptive gravity-balacing system

In order to ensure the balancing of the variable payload, it is necessary to achieve the following modifications to the robot architecture.

First, we slightly modify the robot architecture by adding a revolute joint on the link EF at a new point J defined such that the points B, D and J are aligned (Fig. 3). With the new design, the robot becomes a pantograph linkage [37] with a magnification factor $p = \ell_{EF}/\ell_{EJ}$ which links the position of point D to the position of point J such that:

$$z_D - z_B = p(z_B - z_J) \quad (26)$$

Thanks to this design and the well-kown pantograph properties [38], it is possible to cancel the gravity effect of a mass m applied at point P ($f = m\,g$) by applying a vertical balancing force of magnitude $f_{bal} = p\,g\,m$ at point J.

Then, in order to apply the vertical balancing force at point J, we add the balancing module to the robot (see Fig. 4). This module is made of four joints (three prismatic (*P*) joints located at points K, L and N and one revolute (*R*) joint at point M) and one zero-free length spring of stiffness k_p attached at points T_1 and T_2 with the lengths ℓ_{MT_1} and ℓ_{MT_2} always constant. In this module:

- the *P* joint at point K is passive but it integrates a brake that is activated when the robot is manipulating a constant load and deactivated when the balancing module is adapting to a new payload,
- the *P* joint at point N integrates a motor plus a brake: when the robot manipulates a constant load, the brake is activated and the motor is shut down, while, when the balancing module is adapting to a new payload, the motor is activated and the brake is deactivated,
- the *R* joint at point M and the *P* joint at point L are passive but they integrate brakes that are deactivated when the robot is manipulating a constant load and activated when the balancing module is adapting to a new payload.

This adaptive module is able to ensure the balancing of the variable payload for any robot configuration. Moreover, the adaption does not need to bring additional energy as

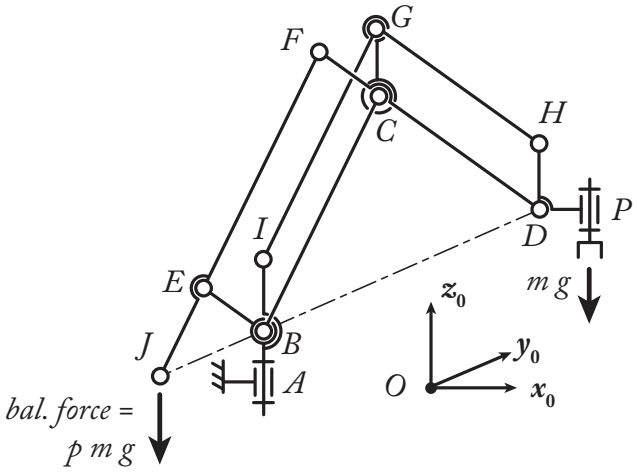

Fig. 3. Modification of the robot architecture so that it becomes a pantograph linkage.

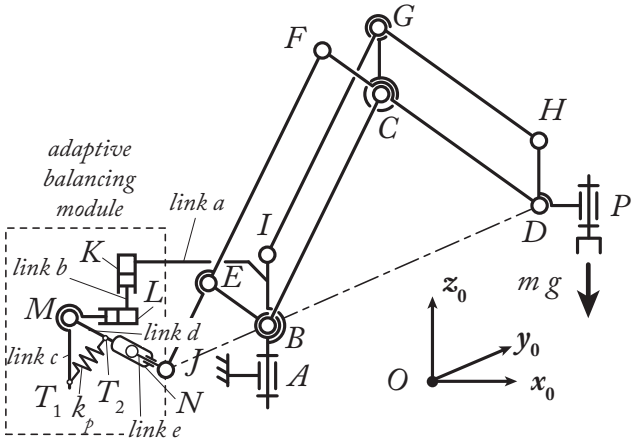

Fig. 4. The robot with the adaptive balancing module.

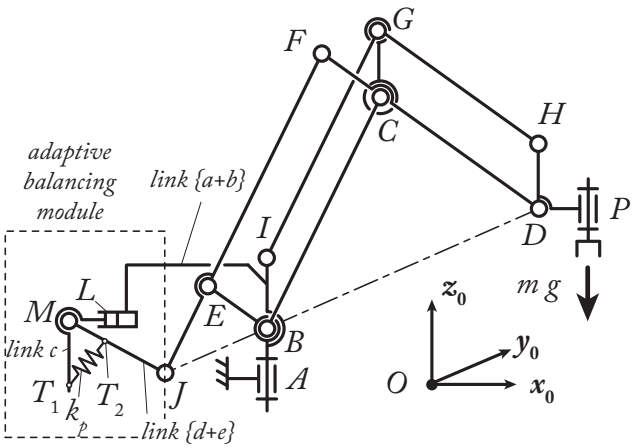

Fig. 5. The robot with the adaptive balancing module and a payload mass m: the *P* joints at points K and N are fixed while the others joints of the adaptive module are passive.

all the requested energy is already stored in the spring of stiffness k_p. In the following sections, we explain how it works.

B. Balancing conditions

B.1 For a payload mass m

As mentioned previously, during the manipulation of a constant payload of mass m, the *P* joints at points K and N are fixed via brakes, while the other joints are passive, and the resulting mechanism is depicted at Fig. 5. When the *P* joints at points K and N are fixed, the balancing module has two planar passive *DOF* which makes it possible to follow the displacement of the point J. Moreover,

- the length ℓ_{MJ} becomes constant and will be denoted as $\ell_{MJ} = \ell_m$,
- the altitude z_M of the point M becomes constant.

Let us show that under certain conditions, the balancing module ensure the gravity compensation of the payload. We define the angle γ as $\gamma \angle T_1 M T_2$ (γ is not constant and depends on the robot configuration). The energy of the zero-free length spring with a stiffness k_p is equal to:

$$V_{bal} = \frac{k_p \ell_{T_1T_2}^2}{2} \tag{27}$$

or also, when considering that $\ell_{T_1T_2}^2 = \ell_{MT_1}^2 + \ell_{MT_2}^2 - 2\ell_{MT_1}\ell_{MT_2}\cos\gamma$

$$V_{bal} = e - k_p \ell_{MT_1}\ell_{MT_2}\cos\gamma \tag{28}$$

where

$$e = \frac{k_p(\ell_{MT_1}^2 + \ell_{MT_2}^2)}{2}$$

For reasons of simplicity of computation, we consider that the centre of mass:

- of the link between points M and N is located at M,
- of the link between points N and J is located at J and has a mass m_J.

Such conditions can be obtained through a proper link design and, eventually, the use of counterweights. Note that these conditions are not necessary, but simplifies the explanation of the ways the balancing module works.

The potential energy of the payload mass plus the balancing module is

$$V_m = m\,g\,z_P + m_J z_J + m_{mod}\,g\,z_M \tag{29}$$

where m_{mod} is the total mass of the links a, b, c and d, and z_M is the constant altitude of the point M.

Noting the fact that $z_P = z_D$ and introducing (26) into (29), we get

$$\begin{aligned} V_m =& m\,g\,(p(z_B - z_J) + z_B) + m_J\,g\,z_J + m_{mod}\,g\,z_M \\ =& h + (m_J - p\,m)\,g\,z_J \end{aligned} \tag{30}$$

with $h = m\,g\,(p+1)z_B + m_{mod}\,g\,z_M = constant$.

Finally, as $z_J = z_M - \ell_{MJ}\cos\gamma = z_M - \ell_m\cos\gamma$, we get

$$\begin{aligned} V_m =& h + (m_J - p\,m)\,g\,(z_M - \ell_m\cos\gamma) \\ =& l + (p\,m - m_J)\,g\,\ell_m\cos\gamma \end{aligned} \tag{31}$$

with $l = h + (m_J - p\,m)\,g\,z_M = constant$.

The balancing module can cancel the gravity effects of the payload mass m if the total potential energy $V_{tot} = V_m + V_{bal}$ is equal to a constant, which can be obtained if and only if (for fixed lengths ℓ_{MT_1}, ℓ_{MT_2} and stiffness k_p):

$$\ell_m = \frac{k_p \ell_{MT_1}\ell_{MT_2}}{(p\,m - m_J)\,g} \tag{32}$$

resulting in $V_{tot} = e + l = constant$.

Thus, by properly fixing the length $\ell_m = \ell_{MJ}$, we can balance the payload mass. Note that in general, $(p\,m - m_J) > 0$, which means that $\ell_m > 0$.

B.2 Adaption to a new payload mass m'

If now we want to balance a payload mass m', by using the equation (32), we see that the length ℓ_{MJ} should adapt to a new constant length ℓ'_m defined as:

$$\ell'_m = \frac{k_p \ell_{MT_1}\ell_{MT_2}}{(p\,m' - m_J)\,g} \tag{33}$$

This adaption can be energy-free by using the following procedure. First, the robot must be stopped at the position the payload should be changed (fig. 6(a)). Thus, the altitude z_P becomes constant. Then, the *R* joint at point M is also fixed while the brake of joint K is deactivated such that the global system is equivalent to the one depicted in Fig. 6. Note that, when the *R* joint at point M is fixed, this

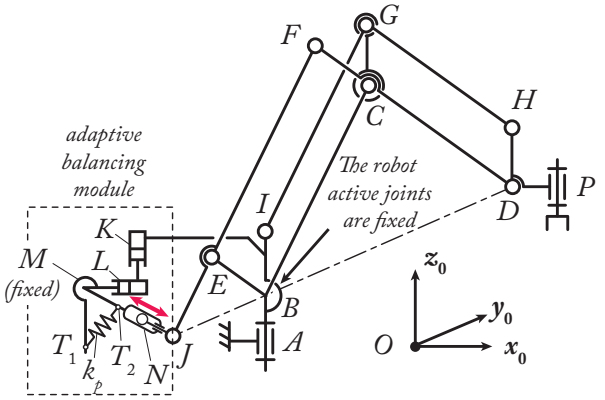

(a)Beginning of the adaption: the robot is stopped. The *P* joint at point K becomes passive while the *R* joint at point M is fixed (thus ensuring the spring potential energy to be stored). The *P* joint at point N is actuated to adapt the length ℓ_{MJ}.

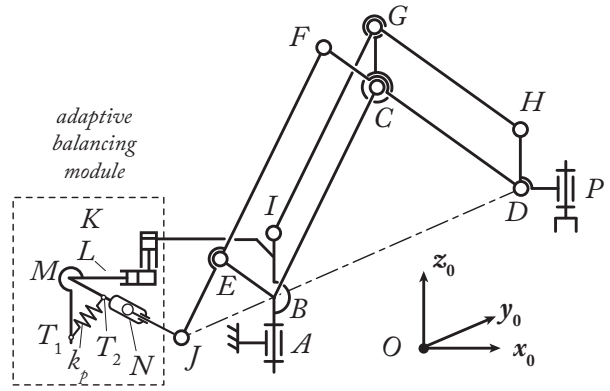

(b)End of the adaption: the system has attained the new length $\ell_{MJ} = \ell'_m$

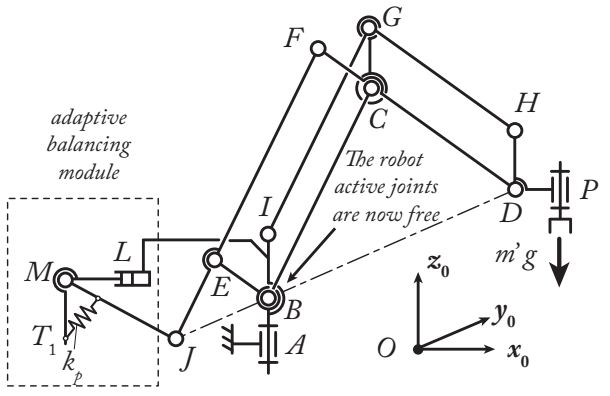

(c)The robot with the adaptive balancing module when manipulating a mass m': the *P* joints at points K and N are fixed while the others joints of the adaptive module are passive.

Fig. 6. Adaption of the balancing system

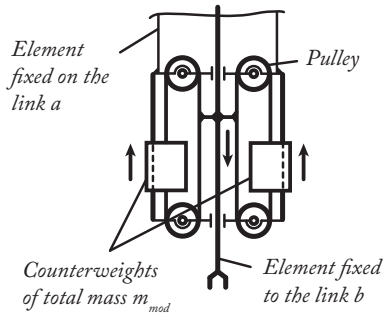

Fig. 7. Balancing device for cancelling the gravity effects due to the mass of the adaptive module: the counterweights are moving in the opposite sense of the link *b* and are thus balancing the moving mass of the gravity-compensation module.

also fix the length $\ell_{P_1P_2}$ of the spring. As a result, during the adaption phase, the spring energy is totally stored (no energy dissipation).

The *P* joints at points K and L are passive while the *P* joint at point N is actuated. A simple mobility analysis shows that the balancing module has thus 1 *DOF* which can be controlled by the actuator in the *P* joint located at point N. This active *P* joint will be used to adapt the length ℓ_{MJ} to become equal to ℓ'_m (Fig. 6(b)).

The robot being fixed, when the active *P* joint is moving, the change of potential energy is only due to the displacement of the links of the balancing module during its adaption. This variation ΔV of energy is equal to:

$$\Delta V = m_{mod}\, g\, \Delta z_M \tag{34}$$

where Δz_M is the variation of altitude of the point M due to the module adaption. This variation of potential energy can be cancelled through a proper balancing system such as the one presented in [39] which is depicted at Fig. 7.

Thus, as the variation of potential energy is null during the adaption phase, the robot does not need (theoretically) any additional energy to adapt to the new payload m', that will be compensated thanks to the optimal adjustment of the length ℓ'_m defined in (33). Once the adaption is done, the robot is gravity-balanced for the new payload m', i.e. the robot actuators do not need to compensate the gravity effects of the mass m' (Fig. 6(c)).

C. Discussion

In the previous Section, it has been mentioned that, during the adaption phase, the robot must be stopped, which will lead to a increase of the operation cycle time. However, in the other techniques [28, 31–35] able to balance a variable load, the robot should also be stopped during the adaption. Thus, stopping the robot is not a drawback due to our balancing technique, but to all adaptive balancing techniques. In order to overcome this drawback, the adaption can be down when the robot is moving. However, this does

not ensure anymore the system to be energy-free during the adaption phase.

Please note also that we claim that the adaption is energy-free. However, we do not take into account the fact that the actuator in the *P* joint located at point N needs energy to move against the friction in the joint. However, our experience in the field has shown that the friction effects are usually very small with respect to the gravity effects which have been compensated.

Finally, the conditions of balancing for the payload described in (32) show that, if $m = 0$, the length ℓ_M should be negative, which is unconvenient from a design point of view. In order to overcome this difficulty, two ways are proposed:

1. we can put a load $m_c > m_J$ on the robot end-effector that will never be removed to ensure that the length ℓ_M will be always positive.
2. it is possible to show in Section II-C that a partial gravity-balancing of the robot architecture can be achieved with counterweights and/or springs so that the potential gravitational energy of the robot becomes a linear function of z_P only, i.e. the robot potential energy has the form $V = m_P\, z_P + constant$, with $m_P > 0$. In such a case, the balancing condition (32) can be rewritten as:

$$\ell_m = \frac{k_p \ell_{MT_1} \ell_{MT_2}}{(p\,(m + m_P) - m_J)\, g} \tag{35}$$

As a result, an optimal design of the robot can ensure that the term $(p\,m + m_P - m_J)$ is always positive.

IV. Numerical validations

In this Section, we present numerical validations made with ADAMS showing that the balancing system is able to compensate a variable payload. We will consider in the following of the Section that the robot is self-balanced by using one of the techniques of Section II. This assumption is made because the paper does not focus on the balancing of the robot itself (which is achieved trough the use of very common techniques which have already been validated in the past) but on the gravity-compensation obtained by the use of the adaptive module.

The simulated robot has the following characteristics:

- the origin of the base frame is at point B, and the point P (position of the end-effector) is superposed with the point D,
- the robot length are: $\ell_{BC} = 1.3$ m, $\ell_{CD} = 1.3$ m, $\ell_{GH} = 1.3$ m, $\ell_{BE} = 0.3$ m, $\ell_{CF} = 0.3$ m, $\ell_{BI} = 0.3$ m, $\ell_{CG} = 0.3$ m and $\ell_{DH} = 0.3$ m.

The gravity-compensation module is designed such that:

- the length ℓ_{EJ} is equal to 0.3 m; as a result, the resulting pantograph mechanism of Fig 3 has a magnification factor $p = 1.3/0.3 \approx 4.33$,
- the total mass of links b, c and d is equal to $m_{mod} = 10$ kg, but is compensated through the addition of the system designed in Fig. 7 with counterweights of total mass equal to 10 kg,
- the total centre of mass of links b, c and d is located at point M,
- the mass of the link e is $m_J = 5$ kg and its centre of mass is located in point J,
- the spring has a stiffness $k_p = 20000$ N/m.

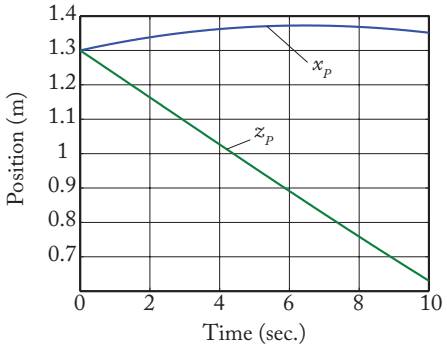

Fig. 8. Trajectory during the manipulation of the payload $m = 100$ kg, defined for $y_P = 0$ m.

First, the robot has to manipulate a payload of mass $m = 100$ kg. As a result, the length ℓ_{MJ} of the module should be equal to $\ell_M = 0.467$ m to balance the gravity effects of the payload m. The payload is manipulated by the robot on the trajectory defined in Fig. 8. The results in terms of robot input torques (Fig. 9) required for manipulating this payload without the gravity-compensation module (full line) and with the gravity-compensation module with the length ℓ_{MJ} equal to $\ell_M = 0.467$ m (dotted line) show that, with the use of the adaptive module, no input torques are required to move the payload.

Then, at the end of the trajectory defined in Fig. 8 (at the point $x_P = 1.35$ m, $y_P = 0$ m and $z_P = 0.63$ m), we change the load and the robot must be able to carry out a mass of $m' = 300$ kg. As a result, the length ℓ_{MJ} of the module should be equal to $\ell'_M = 0.155$ m to balance the gravity effects of the payload m'. We do not show here the variation of potential energy during the process of adaption to the new length because it is equal to zero all the time, i.e. the compensation module does not bring energy to adapt to the new length. The new payload is manipulated by the robot on the trajectory defined in Fig. 10. The results in terms of robot input torques (Fig. 11) required for manipulating this payload without the gravity-compensation module (full line) and with the gravity-compensation module with the length ℓ_{MJ} equal to $\ell_M = 0.467$ m (dotted line) show that, with the use of the adaptive module, no input torques are required to move the payload.

V. Conclusion

In this paper, a new gravity-compensation module for 4-*DOF* robot manipulating variable and heavy loads has been

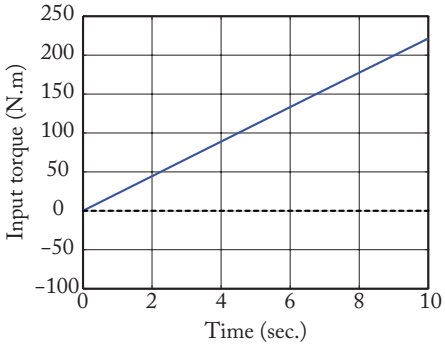

(a)actuator 1

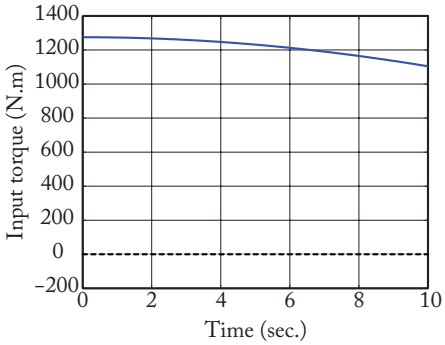

(b)actuator 2

Fig. 9. Input torques for manipulating the payload $m = 100$ kg: without (full line) and with (dotted line) the gravity-compensation module.

proposed. The new balancing scheme allows for the compensation of the gravity effects of the manipulated payload which may vary. Contrary to most of gravity balancing techniques able to compensate the gravity effects of variable loads, this compensation module is energy efficient, i.e. the adaption to the new manipulated payload does not require to bring energy inside the system.

Simulations of the mechanism with ADAMS have been performed and have shown the efficiency of the proposed approach.

Future works will concern the optimal design of a prototype in order to experimentally validate this balancing technique which can find wide applications to the solution of practical problems.

References

[1] G. Dunlop and T. Jones. Gravity counter balancing of parallel robot for antenna aiming. In *Proceedings of the 6th ASRAM*, pages 153–158, 1996.

[2] H. Kazerooni and S. Kim. A new architecture for direct drive robots. In *Proceedings of the IEEE International Conference on Robotics and Automation (ICRA 1988)*, pages 442–445, 1988.

[3] H. Kazerooni. Statically balanced direct drive manipulator. *Robotica*, 7(2):143–149, 1989.

[4] C.M. Gosselin and J. Wang. On the design of gravity-compensated six-degree-of-freedom parallel mechanisms. In *Proceedings of the IEEE International Conference on Robotics and Automation (ICRA 1998)*, pages 2287–2294, Leuven, Belgium, 1998.

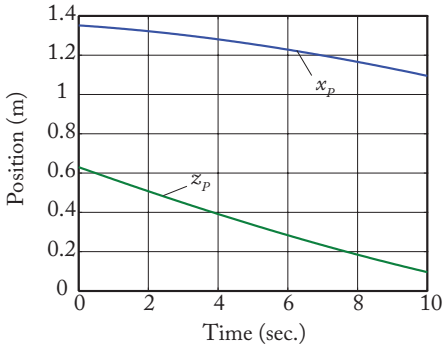

Fig. 10. Trajectory during the manipulation of the payload $m' = 300$ kg, defined for $y_P = 0$ m.

[5] J. Wang and C.M. Gosselin. Static balancing of spatial three-degree-of-freedom parallel mechanisms. *Mechanism and Machine Theory*, 34:437–452, 1999.

[6] W.S. Newman and N. Hogan. the optimal control of balanced manipulators. In *Proceedings of the ASME winter annual meeting*, CA, USA, 1986.

[7] C.M. Gosselin. *Smart Devices and Machines for Advanced Manufacturing*, chapter Gravity compensation, static balancing and dynamic balancing of parallel mechanisms, pages 27–48. Springer, 2008.

[8] J. Wang and C.M. Gosselin. Static balancing of spatial four-degree-of-freedom parallel mechanisms. *Mechanism and Machine Theory*, 35(4):563–592, 2000.

[9] T. Laliberté, C.M. Gosselin, and M. Jean. Static balancing of 3-DOF planar parallel mechanisms. *IEEE/ASME Transactions on Mechatronics*, 4(4):363–377, 1999.

[10] A. Gopalswamy, P. Gupta, and M. Vidyasagar. A new parallelogram linkage configuration for gravity compensation using torsional springs. In *Proceedings of the IEEE International Conference on Robotics and Automation (ICRA 1992)*, pages 664–669, Nice, France, may 1992.

[11] E. Shin and D.A. Streit. Spring equilibrator theory for static balancing of planar pantograph linkages. *Mechanism and Machine Theory*, 26(7):645–657, 1991.

[12] D.A. Streit and E. Shin. Equilibrators for planar linkages. *ASME Journal of Mechanical Design*, 115:604–611, 1993.

[13] T. Rahman, R. Ramanathan, R. Seliktar, and W. Harwin. A simple technique to passively gravity-balance articulated mechanisms. *ASME Journal of Mechanical Design*, 117(4):655–658, 1995.

[14] J.L. Pons, R. Ceres, and A.R. Jiménez. Quasi-exact linear spring counter gravity system for robotic manipulators. *Mechanism and Machine Theory*, 33:59–70, 1998.

[15] C.M. Gosselin. *Computational Methods in Mechanical Systems: Mechanism Analysis, Synthesis, and Optimization*, chapter On the design of efficient parallel mechanisms, pages 68–96. NATO ASI. Springer, Berlin, 1998.

[16] J.L. Herder. Design of spring force compensation systems. *Mechanism and Machine Theory*, 33:151–161, 1998.

[17] I. Ebert-Uphoff, C.M. Gosselin, and T. Laliberté. Static balancing of spatial parallel mechanisms revisited. *ASME Journal of Mechanical Design*, 122:43–51, 2000.

[18] G.J.M. Tuijthof and J.L. Herder. Design, actuation and control of an antropomorphic robot arm. *Mechanism and Machine Theory*, 35:945–962, 2000.

[19] Y. Ono and T. Morita. An underactuated manipulation method using a mechanical gravity canceller. *Journal of Robotics and Mechatronics*, 106(6):563–569, 2004.

[20] P.Y. Lin, W.B. Shieh, and D.Z. Chen. Design of perfectly statically balanced one-DOF planar linkage with revolute joints only. *ASME Journal of Mechanical Design*, 131, 2009.

[21] P.Y. Lin, W.B. Shieh, and D.Z. Chen. A stiffness matrix approach for the design of statically balanced planar articulated manipulators. *Mechanism and Machine Theory*, 45:1877–1891, 2010.

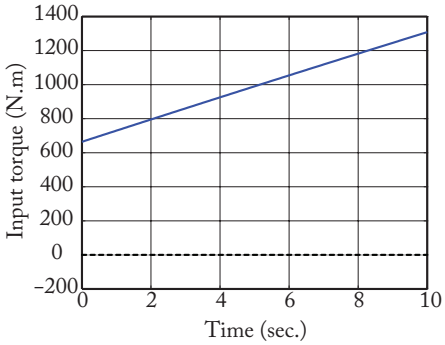

(a)actuator 1

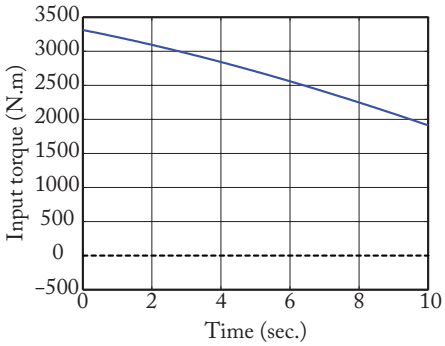

(b)actuator 2

Fig. 11. Input torques for manipulating the payload $m' = 300$ kg: without (full line) and with (dotted line) the gravity-compensation module.

[22] Q. Lu, C. Ortega, and O. Ma. Passive gravity compensation mechanisms: Technologies and applications. *Recent Patents on Engineering*, 5(1):32–44, 2011.

[23] P.Y. Lin, W.B. Shieh, and D.Z. Chen. Design of statically balanced planar articulated manipulator with spring suspension. *IEEE Transactions on Robotics*, 28(1):12–21, 2012.

[24] S.D. Deepak and G.K. Ananthasuresh. Static balancing of a four-bar linkage and its cognates. *Mechanism and Machine Theory*, 48:62–80, 2012.

[25] S.D. Deepak and G.K. Ananthasuresh. Perfect static balancing of linkages by addition of springs but not auxiliary bodies. *ASME Journal of Mechanisms and Robotics*, 4, 2012.

[26] A. Bayer and G. Merk. Industrial robot with a weight balancing system, aug 2011.

[27] P.N. Belyanin. *Balanced manipulators*. Mashinostroyenie, Moscow, 1988.

[28] A. Fahim and M. Fernandez. Performance enhancement of robot arms through active counterbalancing. *International Journal of Advanced Manufacturing Technology*, 3(4):63–72, 1988.

[29] R. Yamamoto, A. Hirakawa, and O. Horikawa. Load balancer with automatic lifting force compensation. In *Proceedings of the ABCM Symposium in Mechatronics*, volume 4, pages 580–589, 2010.

[30] F. Wildenberg. Compensating system for a hexapod. Patent us 6474915, nov 2002.

[31] M. Carricato and C.M. Gosselin. A statically balanced Gough/Stewart-type platform: Conception, design, and simulation. *ASME Journal of Mechanisms and Robotics*, 1, 2009.

[32] N. Takesue, T. Ikematsu, H. Murayama, and H. Fujimoto. Design and prototype of variable gravity compensation mechanism. *Journal of Robotics and Mechatronics*, 23(2):249–257, 2011.

[33] N. Lauzier, C.M. Gosselin, T. Laliberté, and P. Tremblay. Adaptive gravity compensation of decoupled parallel and serial manipulators using a passive hydraulic transmission. *Journal of Mechanical Engineering Science*, 223(12):2871–2879, 2009.

[34] M.A. Lacasse, G. Lachance, J. Boisclair, J. Ouellet, and C.M. Gosselin. On the design of a statically balanced serial robot using remote counterweights. In *Proceedings of the IEEE International Conference on Robotics and Automation (ICRA 2013)*, pages 4174–4179, Karlsruhe, Germany, may 2013.

[35] T. Laliberté, C.M. Gosselin, and D. Gao. Closed-loop actuation routings for cartesian scara-type manipulators. In *Proceedings of the 2010 International Design Engineering Technical Conferences & Computers and Information in Engineering Conference (IDETC/CIE 2010)*, aug 2010.

[36] S. Briot and V. Arakelian. Dispositif déquilibrage de charge pour bras articulé, appareil et procédé de manipulation de charge associé. FR 14 62980, dec 2014. patent pending.

[37] V. Arakelian. équilibrage des manipulateurs manuels. *Mechanism and Machine Theory*, 33(4):437–442, 1998.

[38] S. Briot, V. Arakelian, and S. Guégan. Paminsa: a new family of decoupled parallel manipulators. *Mechanism and Machine Theory*, 44(2):425–444, 2009.

[39] V. Arakelian and S. Briot. Dynamic balancing of the scara robot. In *Proceedings of 17th CISM-IFToMM Symposium on Robot Design, Dynamics, and Control (RoManSy 2008)*, Tokyo, Japan, 2008.